



## Molecular Crystals and Liquid Crystals

Publication details, including instructions for authors and subscription information:

<http://www.tandfonline.com/loi/gmcl16>

### Synthesis, Electrical Conductivity, and Crystal Structure of $(\text{AsPh}_4)_{0.25} [\text{Ni}(\text{dmit})_2]$

Lydie Valade<sup>a</sup>, Jean-Pierre Legros<sup>a</sup>, Patrick Cassoux<sup>a</sup> & Frank Kubel<sup>b a</sup>

<sup>a</sup> Laboratoire de Chimie de Coordination du CNRS, Unité No. 8241 liée par convention à l'université Paul Sabatier, 205 route de Narbonne, 31400, Toulouse, France

<sup>b</sup> Laboratoire de Cristallographie aux rayons X, Université de Genève, 24, Quai E. Ansermet 1211, Genève, 4, Suisse

Version of record first published: 20 Apr 2011.

To cite this article: Lydie Valade, Jean-Pierre Legros, Patrick Cassoux & Frank Kubel (1986): Synthesis, Electrical Conductivity, and Crystal Structure of  $(\text{AsPh}_4)_{0.25} [\text{Ni}(\text{dmit})_2]$ , *Molecular Crystals and Liquid Crystals*, 140:2-4, 335-351

To link to this article: <http://dx.doi.org/10.1080/00268948608080163>

PLEASE SCROLL DOWN FOR ARTICLE

Full terms and conditions of use: <http://www.tandfonline.com/page/terms-and-conditions>

This article may be used for research, teaching, and private study purposes. Any substantial or systematic reproduction, redistribution, reselling, loan, sub-licensing, systematic supply, or distribution in any form to anyone is expressly forbidden.

The publisher does not give any warranty express or implied or make any representation that the contents will be complete or accurate or up to date. The accuracy of any instructions, formulae, and drug doses should be independently verified with primary sources. The publisher shall not be liable for any loss, actions, claims, proceedings, demand, or costs or damages whatsoever or howsoever caused arising directly or indirectly in connection with or arising out of the use of this material.

*Mol. Cryst. Liq. Cryst.*, 1986, Vol. 140, pp. 335–351  
0026-8941/86/1404–0335/\$20.00/0  
© 1986 Gordon and Breach Science Publishers S.A.  
Printed in the United States of America

## Synthesis, Electrical Conductivity, and Crystal Structure of (AsPh<sub>4</sub>)<sub>0.25</sub> [Ni(dmit)<sub>2</sub>]

LYDIE VALADE, JEAN-PIERRE LEGROS and PATRICK CASSOUX

*Laboratoire de Chimie de Coordination du CNRS, Unité No. 8241 liée par  
convention à l'Université Paul Sabatier, 205 route de Narbonne, 31400 Toulouse,  
France*

and

FRANK KUBEL

*Laboratoire de Cristallographie aux rayons X, Université de Genève, 24,  
Quai E. Ansermet, 1211 Genève 4, Suisse*

*(Received March 15, 1986; in final form May 18, 1986)*

The synthesis, conductivity behavior and crystal structure of the ion radical salt (AsPh<sub>4</sub>)<sub>0.25</sub> [Ni(dmit)<sub>2</sub>] are described. This compound crystallizes in the monoclinic system, space group Pn or P2<sub>1</sub>/n,  $a = 13.507(7)$ ,  $b = 6.610(1)$ ,  $c = 44.536(7)$  Å,  $\beta = 96.08(2)^\circ$ . The structure consists of thick layers of stacked Ni(dmit)<sub>2</sub> entities parallel to (001) and separated by AsPh<sub>4</sub><sup>+</sup> cations. Short S . . . S interstack distances are observed such that two-dimensional networks of closely spaced Ni(dmit)<sub>2</sub> are formed in the (001) plane of this structure. The two-dimensional character of the structure is reflected in the low anisotropy in the conductivities measured in the (001) plane ( $\sigma_a : \sigma_b : \sigma_c = 1 : 1 : 10^{-3}$ ). The room-temperature four-probe conductivities measured along the needle axis ( $b$  axis) is  $10\text{--}15 \Omega^{-1} \text{cm}^{-1}$ . Temperature-dependent measurements show a thermally activated conductivity with very low activation energies (ca. 0–0.01 eV).

*Keywords: electrical conductivity, radical salt, two-dimensionality,  
crystal structure, molecular metal, M(dmit)<sub>2</sub> compounds*

### INTRODUCTION

Considerable interest has been recently aroused by the discovery of organic superconductors derived from TMTSF<sup>1–3</sup> or BEDT-TTF.<sup>4–5</sup>

From these works has emerged the understanding of the importance of enhancing interstack interactions as a means of stabilizing the metallic state at low temperature, thus avoiding the metal-to-insulator transition ever encountered on cooling the typical *one-dimensional* molecular metals such as KCP or TTF-TCNQ.

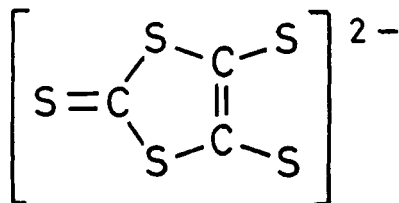
The existence of such interstack interactions results in *two-dimensional* "sheet networks," and this new structural feature is reflected by the low anisotropy in the conductivities observed for these materials, especially (BEDT-TTF)<sub>2</sub>X.<sup>4-5</sup> The use of sulfur (or selenium) atoms on the periphery of the molecule as a means of promoting interstack coupling is a common strategy that has been employed for increasing the dimensionality of molecular metals.<sup>6</sup> Since the early reports on conducting materials derived from the metal complexes of the polysulfur dmit<sup>2-</sup> ligand (H<sub>2</sub>dmit = 4,5-dimercapto-1,3-dithia-2-thione) (Figure 1),<sup>7</sup> and before our recent report on the superconductivity of one of these compounds,<sup>8</sup> these systems have been the subject of a growing number of investigations by several groups.<sup>9-12</sup> We now report the synthesis, electrical conductivity measurements, and structural determination of the mixed-valence salt (AsPh<sub>4</sub>)<sub>0.25</sub>[Ni(dmit)<sub>2</sub>].

The ammonium analogue salts, (n-Bu<sub>4</sub>N)<sub>0.29</sub>[Ni(dmit)<sub>2</sub>]<sup>11</sup> and (Et<sub>4</sub>N)<sub>0.5</sub>[Ni(dmit)<sub>2</sub>]<sup>9a</sup> have been previously described. One of the purposes of this work was to study the influence of the nature of the counteranion upon the stoichiometry and physical properties of such salts. It was also expected that replacing the NR<sub>4</sub><sup>+</sup> cations, which are prone to configurational disorder, by the more rigid AsPh<sub>4</sub><sup>+</sup> cation, could lead to more accurate structural determinations; with regard to the later expectation, the results were deceiving, but for different reasons as will be shown below.

## EXPERIMENTAL

### Syntheses

The dmit<sup>2-</sup> ligand was prepared as previously described.<sup>11b</sup> The (AsPh<sub>4</sub>)<sub>2</sub>[Ni(dmit)<sub>2</sub>] complex was obtained from the dmit(COPh)<sub>2</sub> benzoyl salt, following a procedure similar to that described by Steimecke *et al.*<sup>13</sup> for (NBu<sub>4</sub>)<sub>2</sub>[Ni(dmit)<sub>2</sub>], and substituting the precipitating salt by (AsPh<sub>4</sub>)Cl.<sup>14</sup> Microcrystalline samples thus obtained with 40% yield were characterized by IR spectroscopy (characteristic band frequencies (in cm<sup>-1</sup>): 1430 s (C=C), 1035 and 1015 (C=S), 900 m and 880 sh (C-S), 455 m and 310 m (Ni-S)) and by elemental

FIGURE 1 The  $\text{dmit}^{2-}$  ligand.

analysis (Found: Ni, 4.85; C, 53.10; H, 3.25%.  $[\text{As}(\text{C}_6\text{H}_5)_4]_2 [\text{Ni}(\text{C}_3\text{S}_5)_2]$  requires Ni, 4.82; C, 53.25; H, 3.31%.

Oxidation by air, iodine or bromine yielded sparingly soluble black microcrystalline conducting powders ( $\sigma_{300 \text{ K/compaction}} = 1\text{--}6 \Omega^{-1} \text{ cm}^{-1}$ ). Elemental analysis of these samples gave variable results. However, from these results a stoichiometry  $(\text{AsPh}_4)_x [\text{Ni}(\text{dmit})_2]$  with  $0 < x < 0.5$  can be assigned.

Single crystals of stoichiometry  $(\text{AsPh}_4)_{0.25} [\text{Ni}(\text{dmit})_2]$  were obtained by slow interdiffusion of saturated solutions of  $(\text{AsPh}_4)_2 [\text{Ni}(\text{dmit})_2]$  and  $\text{I}_2/\text{NaI}$  in acetonitrile. Black shiny needles (typically  $2 \times 0.1 \times 0.02 \text{ mm}^3$ ) and platelets ( $2 \times 0.5 \times 0.01 \text{ mm}^3$ ) were isolated by filtration washed with acetonitrile and dried under vacuum. A first indication of the stoichiometry was given by electron microprobe analysis on the crystals (Found: Ni, 10.0%.  $(\text{AsPh}_4)_{0.25} [\text{Ni}(\text{dmit})_2]$  requires Ni, 10.73%). Finally, the needle-like species was characterized by X-ray crystal structure determination as the  $(\text{AsPh}_4)_{0.25} [\text{Ni}(\text{dmit})_2]$  ion radical salt. No X-ray structural determination could be performed on the platelets because of the poor quality of the crystals and extensive twinning. However, approximate cell dimensions close to those of the needle-like crystals have been obtained.

#### Physical measurements

Temperature-dependent (363–77 K) four-probe conductivity measurements were carried out as previously described,<sup>11b</sup> on up to 6 different crystals and gave consistent results. Measurements of the anisotropy in the conductivities in the plane of the largest face of the crystals (001) were carried out using the Montgomery method.<sup>15</sup> The crystals were oriented on an automatic X-ray diffractometer to determine the relationship between the measured conductivities and the crystallographic directions. The conductivity along the third direction [001], was estimated on two-probe mountings (contact resistances, ca. 150  $\Omega$ , were ten times smaller than the bulk resistance of the crystal ca. 1500  $\Omega$ ).

Elemental analyses were performed at the Laboratoire de Chimie de Coordination and at the Service Central de Microanalyse du CNRS. Electron microprobe analysis were performed on a CAMECA, Model MS46 camera. IR spectra were recorded on a Perkin-Elmer, Model 577 spectrophotometer.

### Single crystal X-ray data collection and structure refinement

Crystal data are as follows: black, shiny needles,  $\text{As}_{0.5}\text{Ni}_2\text{S}_{20}\text{C}_{24}\text{H}_{10}$ , molecular weight 1094; monoclinic;  $a = 13.507(7)$ ,  $b = 6.610(1)$ ,  $c = 44.536(7)$  Å,  $\beta = 96.08(2)^\circ$ ;  $V = 3954(3)$  Å<sup>3</sup>;  $Z = 4$ ;  $d_m = 1.83(2)$  (flotation),  $d_{\text{calcd}} = 1.84$  g cm<sup>-3</sup>; space group Pn or P2/n.<sup>16</sup>

The space group was determined from Weissenberg photographs. Diffuse scattering lines observed on the photographs of several crystals indicated propensity toward disorder. This was further confirmed by the first attempts to solve the structure: while the  $\text{Ni}(\text{dmit})_2$  entities could be located, the electronic density cloud between these entities could not be resolved into individual  $\text{AsPh}_4^+$  ions. Finally, a crystal ( $0.64 \times 0.13 \times 0.04$  mm<sup>3</sup>) was found which led to satisfactory structure refinement. Accurate values of the cell parameters were obtained from a least-squares fit to the observed  $\theta$  angles of 20 reflections measured on the diffractometer. Intensity data were collected in the  $\omega/2\theta$  scan mode on a Philips automatic diffractometer using the  $\text{MoK}\alpha$  radiation ( $\lambda = 0.71069$  Å). 3883  $hk \pm 1$  reflections were scanned in the Bragg angle range  $1 < \theta < 18^\circ$  at a constant scan speed of  $1.2^\circ \text{ min}^{-1}$  in  $\omega$ ,  $\omega$  scan width:  $(1.0 + 0.35 \tan \theta)^\circ$ . The intensities of three standard reflections were monitored throughout the data collection and did not show significant variation. A set of 1437 unique observed reflections ( $I > 3\sigma(I)$ ) was used for structure solution and refinement. The usual Lorentz-polarization correction was applied but no correction was made for absorption ( $\mu = 24 \text{ cm}^{-1}$ ).

The structure was solved by the direct methods<sup>17</sup> and the parameters were refined by the full-matrix least-squares technique,<sup>18</sup> assuming the centro-symmetric P2/n space group. The 300 variable parameters included anisotropic temperature factors for the non-carbon atoms and isotropic temperature factors for the carbon atoms. Hydrogen atoms were included at calculated positions ( $d_{\text{C-H}} = 0.97$  Å,  $U = 0.04$  Å<sup>2</sup>) in the final structure factor calculations. The final conventional reliability indices are  $R = \sum |k|F_o| - |F_c| / \sum k|F_o| = 0.049$  and  $R_w = [\sum w(k|F_o| - |F_c|)^2 / \sum w k^2 |F_o|^2]^{1/2} = 0.065$  with  $w = 1/\sigma^2(F_o)$ . The goodness of fit is  $S = [\sum w(k|F_o| - |F_c|)^2 / (\text{NREF} - \text{NV})]^{1/2} = 1.40$ .

Positional parameters of the non-hydrogen atoms are listed in Table I.

TABLE I

Non-hydrogen atom positional parameters. Estimated standard deviations are indicated in parentheses

Atom	<i>x/a</i>	<i>y/b</i>	<i>z/c</i>	Atom	<i>x/a</i>	<i>y/b</i>	<i>z/c</i>
Ni(1)	.8750(2)	.3612(4)	.49583(6)	Ni(2)	.6218(2)	.0915(4)	.48492(5)
S(11)	.8556(4)	.6452(8)	.4723(1)	S(12)	.6233(4)	-.0850(7)	.4444(1)
S(21)	.8754(4)	.1903(8)	.4543(1)	S(22)	.5999(4)	.3732(8)	.4605(1)
S(31)	.8311(4)	.7452(7)	.4055(1)	S(32)	.6058(4)	.0346(7)	.3787(1)
S(41)	.8500(4)	.3229(8)	.3890(1)	S(42)	.5823(4)	.4590(7)	.3934(1)
S(51)	.8142(5)	.6339(9)	.3410(1)	S(52)	.5864(5)	.3381(9)	.3293(1)
S(61)	.8736(4)	.5331(7)	.5373(1)	S(62)	.6423(4)	-.1925(7)	.5084(1)
S(71)	.8961(4)	.0776(7)	.5194(1)	S(72)	.6234(4)	.2643(7)	.5267(1)
S(81)	.9011(4)	.4003(8)	.6027(1)	S(82)	.6678(4)	-.2952(7)	.5747(1)
S(91)	.9211(4)	-.0223(7)	.5860(1)	S(92)	.6510(4)	.1264(8)	.5918(1)
S(101)	.9447(5)	.0910(9)	.6507(1)	S(102)	.6842(5)	-.1943(9)	.6393(1)
C(11)	.850(1)	.574(3)	.4351(4)	C(12)	.608(1)	.095(3)	.4163(4)
C(21)	.861(1)	.374(3)	.4268(4)	C(22)	.597(1)	.292(3)	.4237(4)
C(31)	.833(2)	.570(3)	.3768(5)	C(32)	.590(1)	.280(3)	.3646(4)
C(41)	.893(1)	.346(3)	.5641(4)	C(42)	.649(1)	-.126(3)	.5444(4)
C(51)	.902(1)	.148(3)	.5567(4)	C(52)	.643(1)	.075(3)	.5534(4)
C(61)	.925(1)	.150(3)	.6155(4)	C(62)	.667(1)	-.125(3)	.6043(4)
As	1/4	.1089(4)	1/4	C(107)	.148(1)	.277(3)	.2637(4)
C(101)	.191(1)	-.056(3)	.2174(4)	C(108)	.098(1)	.410(3)	.2423(4)
C(102)	.091(1)	-.055(3)	.2083(4)	C(109)	.022(1)	.523(3)	.2532(5)
C(103)	.053(1)	-.183(3)	.1849(4)	C(110)	.000(1)	.514(3)	.2819(5)
C(104)	.118(1)	-.301(3)	.1713(4)	C(111)	.051(1)	.381(3)	.3026(4)
C(105)	.219(1)	-.308(3)	.1809(4)	C(112)	.125(1)	.267(3)	.2929(4)
C(106)	.258(1)	-.190(3)	.2043(4)				

Atoms are labelled according to Figure 2. Relevant bond lengths and bond angles are listed in Table II. Tables of non-hydrogen atom thermal parameters and hydrogen atom calculated positional parameters have been deposited along with a list of the observed and calculated structure factor amplitudes.<sup>19</sup>

## RESULTS AND DISCUSSION

The room temperature conductivity of several crystals of both forms, measured along the needle axis for the needles and along the longest direction of the (001) face for the platelets, using the four-probe technique, was 10–15 Ω<sup>-1</sup> cm<sup>-1</sup>.

Temperature-dependent measurements over the range 363–77 K show a thermally activated conductivity (Figure 3) for both crystalline forms. The curve of log σ versus 1/*T* is non-linear throughout the entire temperature range investigated. Two different regimes with different activation energies, *Ea*<sub>1</sub> = 0.03 and *Ea*<sub>2</sub> = 0.010 eV, are

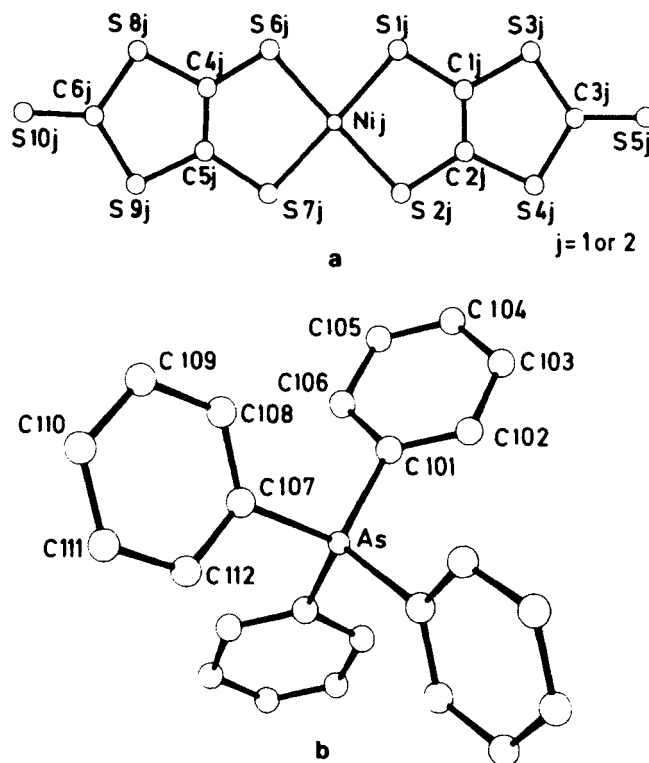


FIGURE 2 Labelling of non-hydrogen atoms in (a) the Ni(dmit)<sub>2</sub> species, and (b) the (AsPh<sub>4</sub>)<sup>+</sup> cation. The digit *j* is used to number the crystallographically independent entities.

observed above and below ca. 150 K, respectively. Thus, the room-temperature conductivity and temperature-dependent behaviour of (AsPh<sub>4</sub>)<sub>0.25</sub> [Ni(dmit)<sub>2</sub>] are very similar to those observed for the previous examples of ion radical salts of Ni(dmit)<sub>2</sub> with *n*-Bu<sub>4</sub>N<sup>+</sup><sup>11</sup> and Et<sub>4</sub>N<sup>+</sup><sup>9a</sup> cations. However, an additional feature is observed on the conductivity curve of (AsPh<sub>4</sub>)<sub>0.25</sub> [Ni(dmit)<sub>2</sub>] in the high temperature range. Above 260 K, the conductivity is nearly constant up to 363 K. In one case (very large needle) a metal-like conductivity behaviour has even been observed above 350 K when increasing the temperature, but this behaviour was not maintained on the subsequent temperature cycles.

The conductivities measured along the *a* and *b* axis by the Montgomery method, and along the *c* axis by the two-probe method, evidenced a quite low anisotropy in the (001) plane:

TABLE II

Bond lengths (Å) and bond angles (°). Estimated standard deviations are  
 Ni—S: .006, C—S: .02, C—C: .03, As—C: .01 Å; S—Ni—S: .2, Ni—S—C: .7,  
 S—C—S: 1., S—C—C: 1., C—S—C: 1., C—As—C: .7, As—C—C: 1.,  
 C—C—C: 2. °. Roman superscript refers to the transformation  $1/2 + x, \bar{y}, 1/2 + z$

As—C(101)	1.918	C(101)—As—C(101) <sup>i</sup>	110.9
As—C(107)	1.916	C(101)—As—C(107)	108.4
		C(101)—As—C(107) <sup>i</sup>	109.9
		C(107)—As—C(107) <sup>i</sup>	109.3
C(101)—C(102)	1.37	As—C(101)—C(102)	122
C(101)—C(106)	1.43	As—C(101)—C(106)	116
C(102)—C(103)	1.40	C(102)—C(101)—C(106)	122
C(103)—C(104)	1.36	C(101)—C(102)—C(103)	120
C(104)—C(105)	1.38	C(102)—C(103)—C(104)	118
C(105)—C(106)	1.36	C(103)—C(104)—C(105)	123
		C(104)—C(105)—C(106)	120
		C(101)—C(106)—C(105)	117
C(107)—C(108)	1.42	As—C(107)—C(108)	117
C(107)—C(112)	1.37	As—C(107)—C(112)	121
C(108)—C(109)	1.40	C(108)—C(107)—C(112)	122
C(109)—C(110)	1.34	C(107)—C(108)—C(109)	115
C(110)—C(111)	1.40	C(108)—C(109)—C(110)	123
C(111)—C(112)	1.36	C(109)—C(110)—C(111)	121
		C(110)—C(111)—C(112)	118
		C(107)—C(112)—C(111)	122
Ni(1)—S(11)	2.152	S(11)—Ni(1)—S(21)	92.9
Ni(1)—S(21)	2.167	S(11)—Ni(1)—S(61)	86.9
Ni(1)—S(61)	2.171	S(21)—Ni(1)—S(71)	87.2
Ni(1)—S(71)	2.153	S(61)—Ni(1)—S(71)	93.1
S(11)—C(11)	1.72	Ni(1)—S(11)—C(11)	102.8
S(21)—C(21)	1.72	Ni(1)—S(21)—C(21)	103.3
S(31)—C(11)	1.74	C(11)—S(31)—C(31)	97
S(31)—C(31)	1.73	C(21)—S(41)—C(31)	97
S(41)—C(21)	1.71	Ni(1)—S(61)—C(41)	101.5
S(41)—C(31)	1.73	Ni(1)—S(71)—C(51)	103.0
S(51)—C(31)	1.64	C(41)—S(81)—C(61)	97
S(61)—C(41)	1.72	C(51)—S(91)—C(61)	98
S(71)—C(51)	1.72	S(11)—C(11)—S(31)	123
S(81)—C(41)	1.75	S(11)—C(11)—C(21)	122
S(81)—C(61)	1.77	S(31)—C(11)—C(21)	115
S(91)—C(51)	1.72	S(21)—C(21)—S(41)	124
S(91)—C(61)	1.74	S(21)—C(21)—C(11)	119
S(101)—C(61)	1.61	S(41)—C(21)—C(11)	117
C(11)—C(21)	1.39	S(31)—C(31)—S(41)	114
C(41)—C(51)	1.36	S(31)—C(31)—S(51)	122
		S(41)—C(31)—S(51)	123
		S(61)—C(41)—S(81)	122
		S(61)—C(41)—C(51)	122
		S(81)—C(41)—C(51)	116
		S(71)—C(51)—S(91)	123
		S(71)—C(51)—C(41)	120
		S(91)—C(51)—C(41)	117
		S(81)—C(61)—S(91)	112
		S(81)—C(61)—S(101)	123
		S(91)—C(61)—S(101)	124



TABLE II *continued*

Ni(2)—S(12)	2.150	S(12)—Ni(2)—S(22)	93.3
Ni(2)—S(22)	2.162	S(12)—Ni(2)—S(62)	85.6
Ni(2)—S(62)	2.153	S(22)—Ni(2)—S(72)	88.1
Ni(2)—S(72)	2.180	S(62)—Ni(2)—S(72)	93.0
S(12)—C(12)	1.72	Ni(2)—S(12)—C(12)	103.0
S(22)—C(22)	1.72	Ni(2)—S(22)—C(22)	101.4
S(32)—C(12)	1.72	C(12)—S(32)—C(32)	97
S(32)—C(32)	1.74	C(22)—S(42)—C(32)	97
S(42)—C(22)	1.74	Ni(2)—S(62)—C(42)	103.4
S(42)—C(32)	1.76	Ni(2)—S(72)—C(52)	101.2
S(52)—C(32)	1.62	C(42)—S(82)—C(62)	99
S(62)—C(42)	1.66	C(52)—S(92)—C(62)	97
S(72)—C(52)	1.73	S(12)—C(12)—S(32)	123
S(82)—C(42)	1.75	S(12)—C(12)—C(22)	119
S(82)—C(62)	1.74	S(32)—C(12)—C(22)	118
S(92)—C(52)	1.74	S(22)—C(22)—S(42)	122
S(92)—C(62)	1.76	S(22)—C(22)—C(12)	123
S(102)—C(62)	1.62	S(42)—C(22)—C(12)	115
C(12)—C(22)	1.35	S(32)—C(32)—S(42)	112
C(42)—C(52)	1.39	S(32)—C(32)—S(52)	124
		S(42)—C(32)—S(52)	123
		S(62)—C(42)—S(82)	125
		S(62)—C(42)—C(52)	122
		S(82)—C(42)—C(52)	113
		S(72)—C(52)—S(92)	122
		S(72)—C(52)—C(42)	120
		S(92)—C(52)—C(42)	118
		S(82)—C(62)—S(92)	113
		S(82)—C(62)—S(102)	122
		S(92)—C(62)—S(102)	125

$\sigma_a : \sigma_b : \sigma_c = 1 : 1 : 10^{-5}$ . This ratio is close to that observed for (*n*-Bu<sub>4</sub>N)<sub>0.29</sub> [Ni(dmit)<sub>2</sub>] ( $\sigma_a : \sigma_b : \sigma_c = 2 : 1 : 10^{-4}$ ),<sup>11b</sup> and for (Et<sub>4</sub>N)<sub>0.5</sub> [Ni(dmit)<sub>2</sub>] ( $\sigma_a : \sigma_b : \sigma_c = 1 : 50 : 8$ ).<sup>9a</sup> Therefore two-dimensionality seems to be a common prominent feature of the conductivity behaviour of Ni(dmit)<sub>2</sub>-based compounds. This observation reflects in the structure of these compounds.

The structure of (AsPh<sub>4</sub>)<sub>0.25</sub> [Ni(dmit)<sub>2</sub>] shows in the asymmetric unit two crystallographically independent Ni(dmit)<sub>2</sub> entities in general positions and one AsPh<sub>4</sub><sup>+</sup> ion lying on a diad axis. The resulting composition is (AsPh<sub>4</sub>)<sub>0.5</sub> [Ni(dmit)<sub>2</sub>]<sub>2</sub>. However, it was more conveniently written as (AsPh<sub>4</sub>)<sub>0.25</sub> [Ni(dmit)<sub>2</sub>] in order to emphasize the fractional oxidation state of the Ni(dmit)<sub>2</sub> species.

The As atoms are located along the diad axis at 1/4, *y*, 1/4 and 3/4,  $\bar{y}$ , 3/4, in such a way that empty tunnels are formed along the diad axis at 3/4, *y*, 1/4 and 1/4,  $\bar{y}$ , 3/4. This empty space may be a good reason for the tendency to disordering mentioned above and for the failure in locating the AsPh<sub>4</sub><sup>+</sup> ions in the first crystals

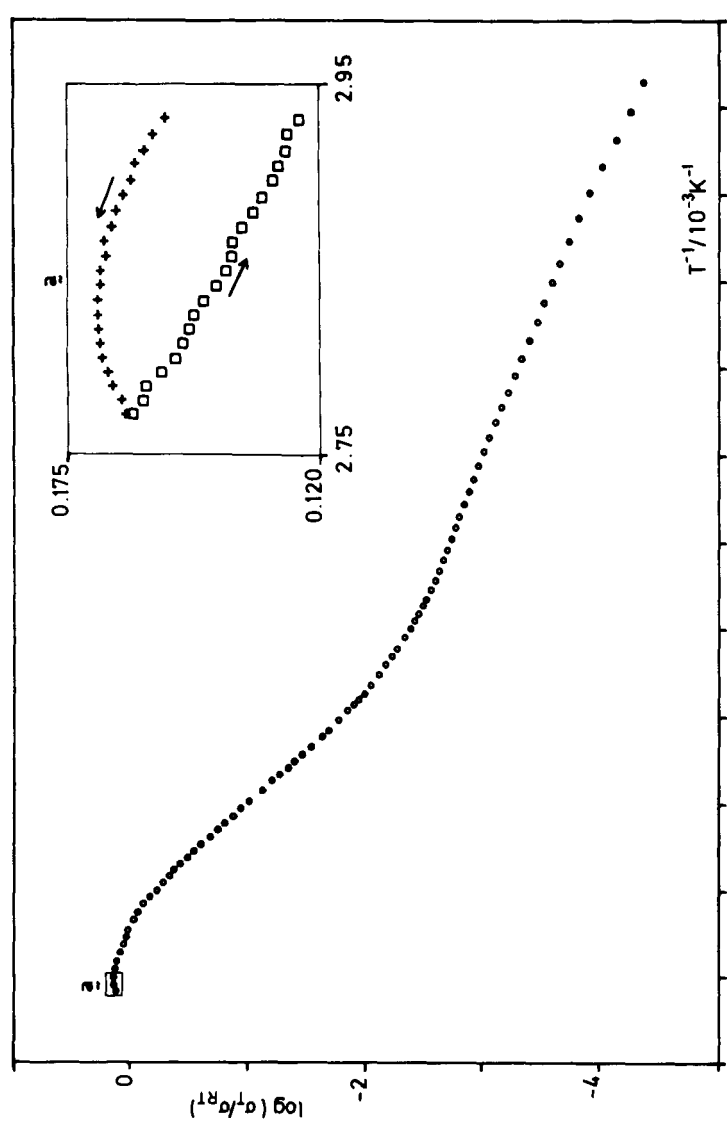


FIGURE 3 Normalized conductivity ( $RT = 285 \text{ K}$ ) of  $(\text{AsPh}_4)_{0.25} [\text{Ni}(\text{dmit})_2]$  as a function of the inverse of temperature. a is a blow-up of the conductivity curve between 340 and 360 K.

studied. The existence of these empty tunnels may also explain the variable analysis data obtained when characterizing the various chemical phases obtained by oxidation of  $(\text{AsPh}_4)_2 [\text{Ni}(\text{dmit})_2]$ . Actually, this space may be filled with variable amounts of  $\text{AsPh}_4^+$  ions and could even be used to insert other redox species, thus possibly varying the partial oxidation state of the  $\text{Ni}(\text{dmit})_2$ . The ability of the  $\text{Ni}(\text{dmit})_2$  species to reach variable overall oxidation states is also reflected by the different stoichiometries obtained for the  $\text{Et}_4\text{N}^+$  and  $n\text{-Bu}_4\text{N}^+$  salts.

All the nickel atoms of  $(\text{AsPh}_4)_{0.25} [\text{Ni}(\text{dmit})_2]$  lie close to the  $z = 0$  and  $z = 1/2$  planes. The structure can thus be described as consisting of thick layers of  $\text{Ni}(\text{dmit})_2$  entities parallel to (001) and separated by the  $\text{AsPh}_4^+$  cations (Figure 4). Within the layer the  $\text{Ni}(\text{dmit})_2$  species are arranged in stacks; the stacking direction is alternately  $[110]$  at the level  $z \sim 0$  and  $[110]$  at the level  $z \sim 1/2$ . A stack consists of quasi-parallel quasi-planar  $\text{Ni}(\text{dmit})_2$  entities<sup>19</sup> arranged in tetrads (Figure 5). The interplanar distances within a tetrad are 3.53 and 3.50 Å and compare well with the regular stacking distance (3.55 Å) in the low-temperature metallic conductor TTF  $[\text{Ni}(\text{dmit})_2]_2$ .<sup>12a</sup> Non-regular stacking arrangements have also been observed in the related  $n\text{-Bu}_4\text{N}^+$  and  $\text{Et}_4\text{N}^+$  salts: alternating triads and tetrads in the former and diads in the latter. The interplanar distances range from 3.48 to 3.57 Å within the triads and tetrads and are 3.44 Å within the diads. On the basis of the interplanar distances, the  $\text{Ni}(\text{dmit})_2$  units appear more strongly coupled in the diads of  $(\text{Et}_4\text{N})_{0.5} [\text{Ni}(\text{dmit})_2]$  than in the triads and tetrads of  $(n\text{-Bu}_4\text{N})_{0.29} [\text{Ni}(\text{dmit})_2]$  and in the tetrads of  $(\text{AsPh}_4)_{0.25} [\text{Ni}(\text{dmit})_2]$ . This is supported by the comparison of the distances between the diad-, triad-, and tetrad-blocks within a stack; in the  $\text{Et}_4\text{N}^+$  salt, the diads are separated by 3.76 Å while the inter-group distances are 3.53 and 3.57 Å in the  $n\text{-Bu}_4\text{N}^+$  salt and 3.61 Å in the  $\text{AsPh}_4^+$  salt.

The overlap of the molecules within a tetrad of the  $\text{AsPh}_4^+$  salt is drawn on Figure 6a and b. It is characterized by a transverse offset which gives a sulfur-over-ring pattern. Between two tetrads, the overlap can be described as a longitudinal offset giving a metal-over-ring pattern (Figure 6c). This can be viewed as a shearing in the stacking arrangement.

In addition to the strong  $\pi$  interactions evidenced by the short intrastack distances, there is a number of close S . . . S intermolecular interactions. Table III lists the intermolecular S . . . S distances shorter than the sum of the Van der Waals radii (3.7 Å).<sup>20</sup> It should be pointed out that all but one of the listed distances refer to *interstack* contacts.

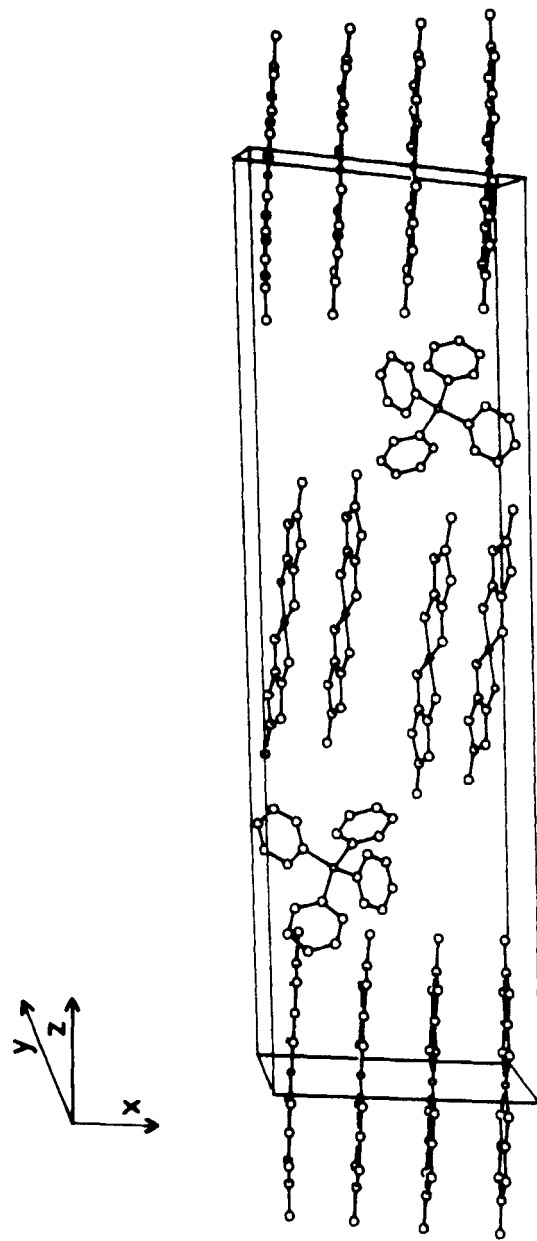


FIGURE 4 Perspective view of the molecular packing.

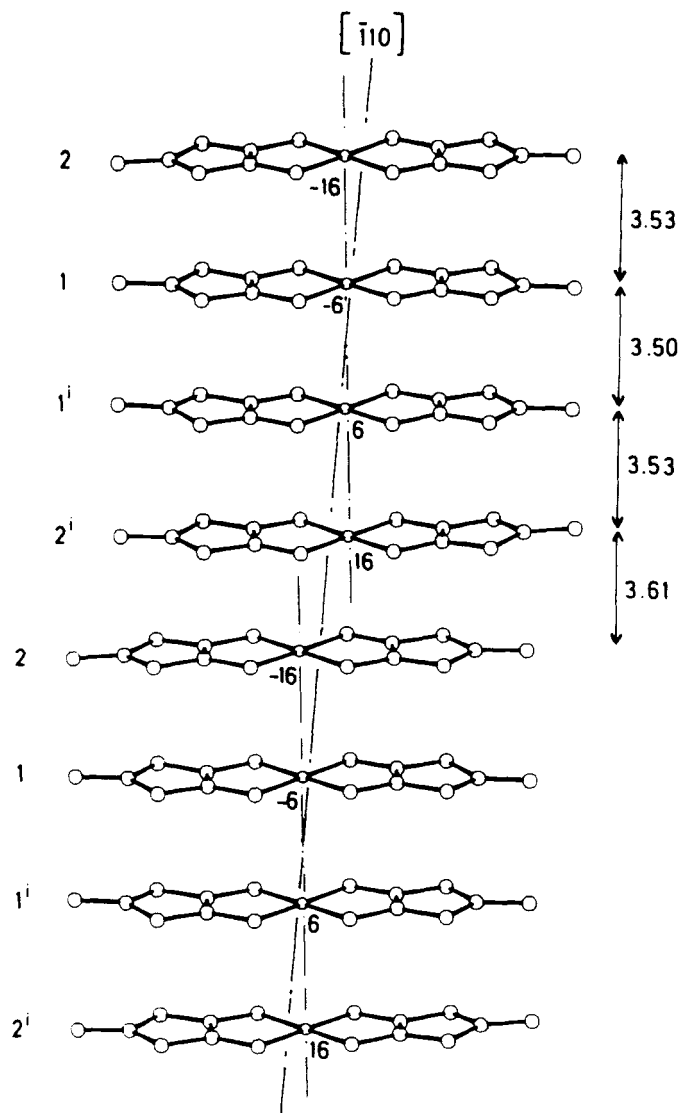


FIGURE 5 Orthogonal projection of a stack onto a plane defined by the stacking direction  $[110]$  and the molecular axis S(51)—S(101). The level of the Ni atoms above this plane is indicated in arbitrary units. Interplanar distances in Å. Number 1 and 2 refer to Ni(1) and Ni(2) respectively and superscript  $i$  indicates symmetry through a centre of inversion.

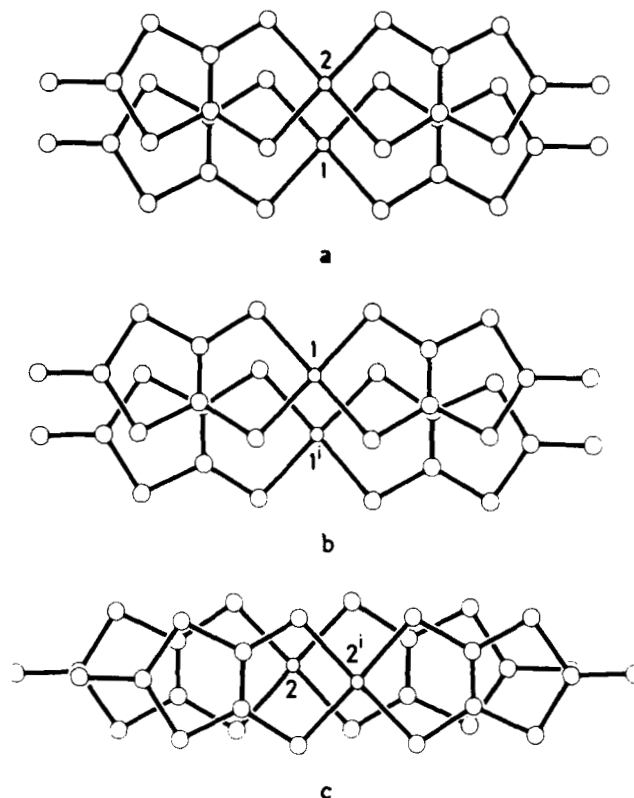


FIGURE 6 Overlap of  $\text{Ni}(\text{dmit})_2$  entities within a tetrad (*a*, *b*) and between two tetrads (*c*). Number 1 and 2 refer to Ni(1) and Ni(2), respectively, and superscript *i* indicates symmetry through a centre of inversion.

Because of tetramerization these S . . . S contacts occur in strips involving adjacent tetrads and running along  $[010]$  (Figure 7). As a consequence of the shearing in the stacking arrangement mentioned above, these strips are loosely connected through S . . . S contacts of 3.8–3.9 Å which cannot be neglected. Thus, the S . . . S network, parallel to the (001) plane, is mainly two-dimensional in nature. In spite of different stacking arrangements, the parent ammonium salts show similar two-dimensional S . . . S networks characterized by the predominance of interstack interactions.

This common structural feature directly accounts for the two-dimensional character of the conductivities in the  $C_x [\text{Ni}(\text{dmit})_2]$  ( $C = \text{Et}_4\text{N}^+$ ,  $n\text{-Bu}_4\text{N}^+$ ,  $\text{AsPh}_4^+$ ) series. However, while bulky ions such as  $n\text{-Bu}_4\text{N}^+$  and  $\text{AsPh}_4^+$  form strong barriers which prevent

TABLE III

Intermolecular S . . . S interactions larger than 3.7 Å. Estimated standard deviation is 0.01 Å. Intrastack interaction is flagged with a star. Roman superscripts refer to the following transformations:

$$\text{i} \quad x, 1 + y, z$$

$$\text{ii} \quad x, y - 1, z$$

S(11) . . . S(71) <sup>i</sup>	3.55
S(21) . . . S(31) <sup>ii</sup>	3.67
S(61) . . . S(91) <sup>i</sup>	3.67
S(11) . . . S(62) <sup>i</sup>	3.61
S(31) . . . S(12) <sup>i</sup>	3.63
S(31) . . . S(32) <sup>i</sup>	3.69
*S(51) . . . S(52)	3.64
S(61) . . . S(82) <sup>i</sup>	3.57
S(12) . . . S(22) <sup>ii</sup>	3.67
S(22) . . . S(62) <sup>i</sup>	3.59
S(72) . . . S(82) <sup>i</sup>	3.62

conduction in the third direction (perpendicular to the Ni(dmit)<sub>2</sub>-containing layers), the smaller Et<sub>4</sub>N<sup>+</sup> cation allows a low conduction in this direction. This is related to weak interactions between terminal S atoms (S . . . S = 3.9 Å) of Ni(dmit)<sub>2</sub> units located in adjacent layers. The Et<sub>4</sub>N<sup>+</sup> salt is thus considered as a "precursor of a three-dimensional molecular metal."<sup>9a</sup> Such a tendency may be even enhanced when replacing Et<sub>4</sub>N<sup>+</sup> by a sulfur-containing donor molecule: in TTF [Ni(dmit)<sub>2</sub>]<sub>2</sub>, the two-dimensional Ni(dmit)<sub>2</sub> layers are linked by the TTF units so as to provide a quasi-three-dimensional network of intermolecular S . . . S interactions.<sup>12a</sup>

Several conclusions may be drawn from this discussion:

- (i) the oxidation state of the Ni(dmit)<sub>2</sub> species and, correlatively, the crystal structure of the related ion radical salts, are strongly dependent on the nature of the cation;
- (ii) however, all three salts are characterized by the two-dimensionality of the S . . . S interactions network and, as a consequence, display low anisotropy in the conductivities;
- (iii) a small cation may favour an increase of the dimensionality of the system; however, the use of a sulfur-containing cation seems to be a better strategy.

## SUPPLEMENTARY MATERIAL

Tables of non-carbon atom anisotropic thermal parameters, carbon-atom isotropic thermal parameters, hydrogen atom calculated

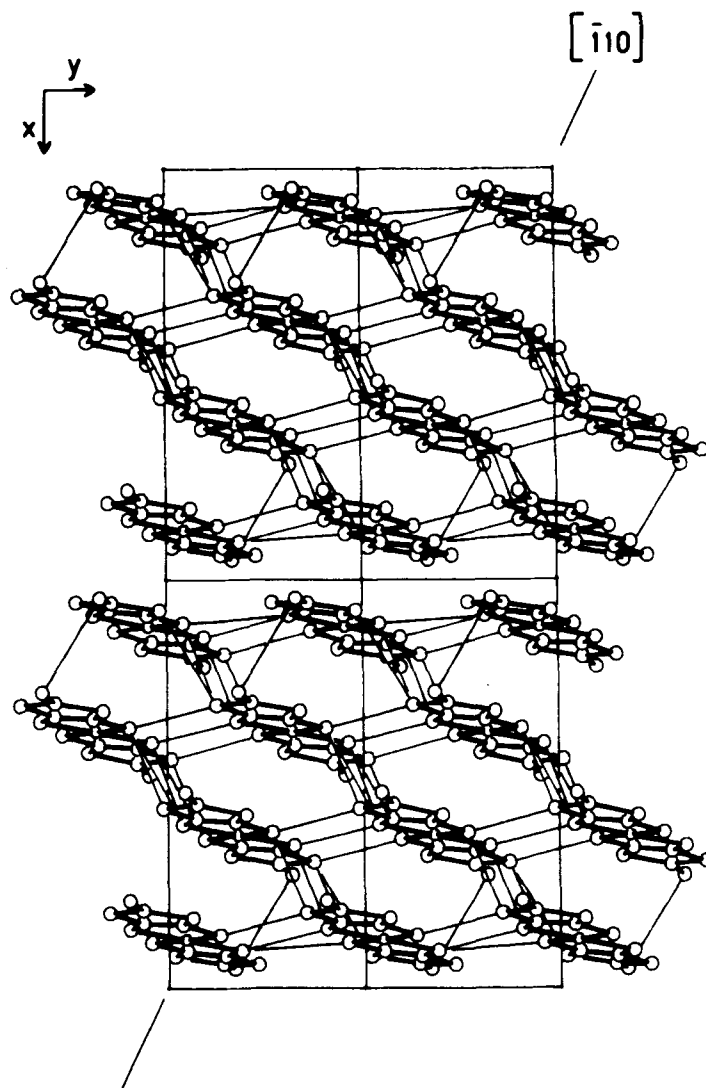


FIGURE 7 Intermolecular S . . . S interactions (thin lines). Projection onto the (001) plane, tilted by  $+10^\circ$  around the  $y$  axis. Four unit cells are drawn.

positional parameters, observed and calculated structure factor amplitudes, and deviations of atoms from their least-squares plane have been deposited. This material may be obtained by contacting Gordon and Breach, P.O. Box 786 Cooper Station, New York, NY 10276.



### Acknowledgments

We are grateful to the NATO Scientific Affairs Division for the support of this work. We thank Dr. J. Galy for his interest in this work and for the facilities he offered. We also thank P. Lecante for great help in computer monitored conductivity experiments and data processing.

### References

1. (a) K. Bechgaard, C. S. Jacobsen, K. Mortensen, H. J. Pedersen and N. Thorup, *Solid State Commun.*, **33**, 1119–1125 (1980); (b) D. Jerome, A. Mazaud, M. Ribault and K. Bechgaard, *J. Phys. (Paris), Lett.*, **41**, L95–L97 (1980).
2. (a) K. Bechgaard, K. Carneiro, F. B. Rasmussen, M. Olsen, G. Rindorf, C. S. Jacobsen, H. J. Pedersen and J. C. Scott, *J. Am. Chem. Soc.*, **103**, 2440–2442 (1981); (b) K. Bechgaard, K. Carneiro, M. Olsen, F. B. Rasmussen and C. S. Jacobsen, *Phys. Rev. Lett.*, **46**, 852–855 (1981).
3. (a) F. Wudl, *J. Am. Chem. Soc.*, **103**, 7064–7069 (1981); (b) G. Rindorf, H. Soling and N. Thorup, *Acta Crystallogr., Sect. B.*, **B38**, 2805–2808 (1982); (c) M. A. Beno, J. M. Williams, M. M. Lee and D. O. Cowan, *Solid State Commun.*, **44**, 1195–1198 (1982).
4. (a) E. B. Yagubskii, I. F. Shchegolev, V. N. Laukhin, P. A. Kononovich, M. V. Karatsovnik, A. V. Zvarykina, L. I. Buravov, *Pis'ma Zh. Eksp. Teor. Fiz.*, **39**, 12–15 (1984). (*J.E.T.P. Lett.*, **39**, 12–16 (1984)); (b) G. Saito, T. Enoki, K. Toriumi, H. Inokuchi, *Solid State Commun.*, **42**, 557–560 (1982).
5. (a) V. F. Kaminski, T. G. Prokhorova, R. P. Shibaeva, E. B. Yagubskii, *Pis'ma Zh. Eksp. Teor. Fiz.*, **39**, 15–18 (1984). (*J.E.T.P. Lett.*, **39**, 17–20 (1984)); (b) H. Kobayashi, A. Kobayashi, Y. Sasaki, G. Saito, T. Enoki, H. Inokuchi, *J. Am. Chem. Soc.*, **105**, 297–298 (1983); (c) J. M. Williams, T. J. Emge, H. H. Wang, M. A. Beno, P. T. Copps, L. N. Hall, K. D. Carlson, G. W. Crabtree, *Inorg. Chem.*, **23**, 2560–2561 (1984); (d) J. M. Williams, H. H. Wang, M. A. Beno, T. J. Emge, L. M. Sowa, P. T. Copps, F. Behrooz, L. N. Hall, K. D. Carlson, G. W. Crabtree, *Inorg. Chem.*, **23**, 3839–3841 (1984).
6. F. Wudl, *Pure Appl. Chem.*, **54**, 1051–1058 (1982).
7. (a) J. Ribas and P. Cassoux, *C.R. Acad. Sci. Paris, Série II*, **283**, 287–290 (1981); (b) G. C. Papavassiliou, *Z. Naturforsch.*, **36b**, 1200–1204 (1981); (c) *ibid.*, **37b**, 825–827 (1982).
8. L. Brossard, M. Ribault, M. Bousseau, L. Valade and P. Cassoux, *C.R. Acad. Sc., Paris, Série II*, **302**, 205–210 (1986).
9. (a) R. Kato, T. Mori, A. Kobayashi, Y. Sasaki and H. Kobayashi, *Chem. Lett.*, 1–4 (1984); (b) R. Kato, H. Kobayashi, A. Kobayashi and Y. Sasaki, *ibid.*, 131–134 (1985); (c) H. Kobayashi, R. Kato, A. Kobayashi and Y. Sasaki, *ibid.*, 191–194 (1985); (d) H. Kobayashi, R. Kato, A. Kobayashi and Y. Sasaki, *ibid.*, 535–538 (1985).
10. N. Thorup and G. Rindorf, *Ninth European Crystallographic Meeting*, Torino, (1985), Abstracts, p. 513.
11. (a) L. Valade, P. Cassoux, A. Gleizes and L. Interrante, *J. Chem. Soc. Chem. Commun.*, 110–112 (1983); (b) L. Valade, J.-P. Legros, M. Bousseau, P. Cassoux, M. Garbauskas and L. V. Interrante, *J. Chem. Soc. Dalton Trans.*, 783–794 (1985).
12. (a) M. Bousseau, L. Valade, J.-P. Legros, P. Cassoux, M. Garbauskas and L. Interrante, *J. Am. Chem. Soc.*, **108**, 1908–1916 (1986); (b) L. Valade and P. Cassoux, *C.R. Acad. Sci. Paris, Série II*, **301**, 999–1002 (1985); (c) J.-P. Ulmet, P. Auban, A. Khmou, L. Valade and P. Cassoux, *Phys. Lett.*, **113A**, 217–219 (1985).

13. G. Steimecke, H. J. Sieler, R. Kirmse and E. Hoyer, *Phosphorus and Sulfur*, **7**, 49–55 (1979).
14. L. Valade, “3ème Cycle,” D. thesis, Toulouse III, (1983).
15. H. C. Montgomery, *J. Appl. Phys.*, **42**, 2971–2975 (1971).
16. Pn and P2/n are non standard settings of space groups number 7 and 13 respectively; reflection conditions:  $h01: h + 1 = 2n$ ; general position coordinates for P2/n  $\pm (x, y, z; x + 1/2, \bar{y}, z + 1/2)$ . International Tables for Crystallography, Vol. A, International Union of Crystallography, D. Reidel Pub., (1983).
17. P. Main, S. E. Hull, L. Lessinger, G. Germain, J.-P. Declercq and M. H. Woolfson, *MULTAN 78*, a system of computer programs for the automatic solution of crystal structures from X-ray diffraction data, Univs. of York, England and Louvain, Belgium, (1978).
18. J. M. Stewart, P. A. Machin, C. W. Dickinson, H. L. Ammon, H. Heck and H. D. Flack, *The X-ray 76 System; Technical report N° TR-446*, Computer Science Center, University of Maryland, College Park, Maryland, (1976).
19. Supplementary Material.
20. L. Pauling, “*The Nature of the Chemical Bond*,” Cornell University Press, Ithaca, New York, (1960).